ment is not too surprising for this particular alloy system because the magnetic scattering time (10^{-11} sec) is much longer than the nonmagnetic scattering time (10^{-14} sec), and we know from susceptibility measurements that the Gd ions are paramagnetic. These are exactly the conditions for the application of the AG theory. No attempt is made to compare with the Gruenberg theory,[3] because the spin-scattering time is too long.

In order to make a direct quantitative comparison with the theory, we used the measured value of the alloy transition temperature T_c and the pure-metal transition temperature T_{cp} in conjunction with the theory to calculate the lifetime broadening, the order parameter, and the thermal conductivity. Details of this sort of calculation are given elsewhere.[8] Results for both the theory (solid line) and experiment (open circle) are shown in Figs. 7 and 8. This must be considered to be very good agreement providing one can assume that the addition of magnetic impurity does not change the phonon contribution.

CONCLUSION

From this work and the earlier equilibrium measurements[8] we conclude that the Abrikosov-Gorkov theory[15] (and its extension to transport properties by Ambegaokar and Griffin) of superconductors containing paramagnetic impurities describes both the equilibrium and transport properties of Th-Gd alloys to a very high accuracy. Not only is the theory qualitatively correct, but it is quantitatively correct to a few percent.

[15] A. A. Abrikosov and L. P. Gorkov, Zh. Eksperim. i Teor. Fiz. **39**, 178 (1960) [English transl.: Soviet Phys.—JETP **12**, 1243 (1961)].

PHYSICAL REVIEW VOLUME 188, NUMBER 2 10 DECEMBER 1969

Elastic Properties of Superconductors: Nb, V, and Ta†

G. W. GOODRICH* AND J. N. LANGE
Department of Physics, Oklahoma State University, Stillwater, Oklahoma 74074

(Received 17 July 1969)

The magnetic field dependence of Young's modulus of type-I and type-II superconductors is used to study the properties of the intermediate and mixed states. The density and separation of vortices in the mixed state are computed from the observed field dependence of the elasticity by use of a model which allows the vortex to expand. A residual stiffness associated with trapped flux is observed to decrease at lower temperatures as a result of reduced pinning forces acting on the vortices. The pinning forces appear to be associated with more than elastic coupling done to the imperfections. The largest total change in stiffness due to the superconducting transition is associated with the longest normal-electron mean free path. Shielding of the lattice initeractions in the superconductng state appears to be more effective the longer the coherence of the superconducting pairs between scatterings. Use of elastic measurements as a means of determining bulk characteristics of the superconductor is found to be quite accurate for materials with low acoustic losses. Anisotropies in the bulk critical fields of niobium are determined simultaneously with the magnetization.

INTRODUCTION

THE elastic properties of solids are modified by the transition to the superconducting state. An early success of the Bardeen-Cooper-Schriefer theory of superconductivity resulted from its ability to predict the temperature dependence of the ultrasonic attenuation, which has since become a standard technique to determine energy gaps of superconducting solids. Changes in the stiffness of a solid entering the superconducting state are much smaller than those of the attenuation. Experimental techniques of high accuracy are needed to observe the transition. Observations of these elastic changes were first made in tin.[1–3] Ensuing work by Alers and Waldorf[4,5] also considered type-II superconductors. Recent investigations by Kramer and Bauer have determined both the temperature[6] and magnetic field[7] dependence of the elasticity in superconducting Nb.

† Work supported by the National Science Foundation.
* Submitted in partial fulfillment of requirements for the Ph.D. degree at the Oklahoma State University.

[1] J. K. Landaver, Phys. Rev. **96**, 296 (1954).
[2] B. Welber and S. L. Quimby, Acta Met. **6**, 351 (1958).
[3] D. F. Gibbins and C. A. Renton, Phys. Rev. **114**, 1257 (1969).
[4] G. A. Alers and D. L. Waldorf, Phys. Rev. Letters **6**, 677 (1961).
[5] G. A. Alers and D. L. Waldorf, IBM J. Res. Develop. **6**, 89 (1962).
[6] E. J. Kramer and C. L. Bauer, Phys. Rev. **163**, 407 (1967).
[7] E. J. Kramer and C. L. Bauer, Phys. Status Solidi **22**, 199 (1967).

The purpose of this investigation is to use the magnetic field dependence of the elasticity to obtain information concerning the intermediate state in type-I materials and the mixed state in type-II materials. Since the elasticity is a bulk property of the solid, its behavior in the superconducting state as a function of magnetic field provides information on the internal state of the solid. The high accuracy of measurement attainable with high-Q materials offers convenient means of determining the magnitudes and anisotropies of the bulk critical fields.

The magnetic field dependence of the elasticity of type-I materials in the intermediate state appears to depend only on the volume of normal material which exists in a noninteracting configuration. The field dependence of the elasticity of type-II materials in the mixed state is considerably more complicated and indicates that interactions between vortices are significant. A calculation based on the model of the vortex suggested by Caroli, de Gennes, and Matricon[8] is used in conjunction with the observed elastic changes to determine the density and size of interacting vortices as a function of applied field.

The change in elasticity resulting from a superconducting transition results from the coherent shielding of lattice-ion interactions by superconducting quasiparticles. The magnitude of these elastic changes in both type-I and type-II materials is observed to be dependent on the mean free path of the normal electrons. The larger elastic changes being associated with the longer mean free paths suggests that the longer the coherence of the unscattered quasiparticles, the more effective is the shielding.

A residual stiffness resulting from flux trapped in the bulk of the material exhibits a temperature dependence which indicates the pinning forces involve more than elastic interactions.

EXPERIMENTAL PROCEDURE

The magnetic field dependence of the complex elasticity (stiffness and attenuation) of a superconducting solid is determined by a standing-wave technique. The relative magnetization is also measured simultaneously by a set of coils fixed near the resonating specimen. The magnetic field dependence of the elasticity is determined from measurement of the fundamental longitudinal resonant frequency as a function of field at a fixed temperature. The change in length of the specimen due to the transition to the normal state has a negligible effect on the resonant frequency compared with the observed elastic changes. The attenuation is determined from the time rate of decay of the standing wave when the driving voltage is switched off. The specimen is a rod of circular cross section, the dimensions of which are chosen to provide a fundamental longitudinal resonant frequency of 30–50 kHz. The specimen is supported at its midplane, which is a node for the fundamental longitudinal mode, and acoustically driven by the force developed between two parallel capacitor plates when the applied voltage is changed.[9] The plane end of the specimen is one of the parallel-plate capacitors whose vibrational motion is monitored by an FM receiver using the capacitor as part of its tank circuit.

FIG. 1. Specimen is suspended by four pins in the nodal plane for the fundamental longitudinal mode. Excitation is through a capacitive drive, for which one plane end of the specimen forms a plate. Detection of the vibration amplitude uses the same capacitor as part of an FM detector similar to the arrangement of Bordoni. The relative magnetization is determined from the voltage in the two coils near the end of the specimen. The coils are connected in opposition similar to the arrangement of Foner and the field vector is always oriented in a plane containing the axes of the coils. The coil voltage is monitored by a phase-sensitive detector.

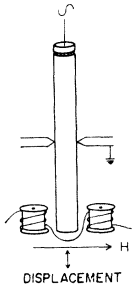

The resolution of the resonant frequency and, thus, the elasticity, is determined by the width of the resonant peak which in turn reflects the attenuation of the entire system. Extraneous attenuation is minimized through reducing sound radiation from the specimen by operating at ambient pressures of 500 μ and by using a suspension consisting of four rigidly mounted pins which support the specimen in a nodal plane. This reduces the relative motion between the specimen and the mount and minimizes its contribution to the attenuation. Further reductions in the attenuation result from removing imperfections and impurities from the specimen surface by etching in acid. Annealing at temperatures much below the melting point decreases the attenuation substantially in Nb without affecting the superconducting critical fields or the resistivity ratio. Very small attenuation is observed in Nb after it is subjected to these procedures such that a decrease in vibration amplitude of 60 dB takes over 2 min. The resulting bandwidth at the half-power points is the order of five thousandths of a cycle, allowing a resolution of better than $\frac{1}{2}$ppm change in elasticity.

The external magnetic field is applied in a plane perpendicular to the axis of the cylinder and can be rotated about this axis. The field is homogeneous to less than $\frac{1}{3}$ of a part in a thousand along the linegth of the specimen. The orientation of the magnetic field leads to a demagnetizing factor of $\frac{1}{2}$ in., and an intermediate state in type-I superconductors is observed. The experimental arrangement is shown in Fig. 1, including the two coils used to determine the relative magnetization. The axis of the coils form a plane containing the magnetic field vector. The coils, 600 turns of copper wire, are connected in opposition to cancel coherent signals induced by an external source.

[8] C. Caroli, P. G. de Gennes, and J. Matricon, Phys. Letters **9**, 309 (1964).

[9] P. G. Bordoni, J. Acoust. Soc. Am. **26**, 495 (1954).

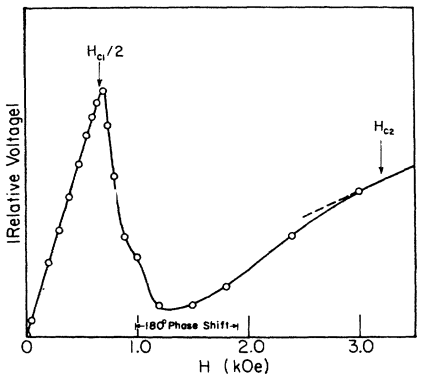

FIG. 2. Relative magnetization of Nb determined by using the coil arrangement of Fig. 1. The perfectly diamagnetic region is shown by a linear increase in the magnetization to a field of one-half the first critical field (demagnetization factor for H perpendicular to the cylinder axis is $\frac{1}{2}$). The net magnetization decreases as the flux penetrates the material in the intermediate state. Above H_{c1} another linearly increasing signal, which is 180° out of phase with the diamagnetic signal, results from the Lorentz currents generated by the acoustic vibration of the rod in the magnetic field.

In the Meissner state the cylinder is perfectly diamagnetic and an external dipole field is introduced in the direction of the applied field. The dipole moves as a result of the vibrational motion of the specimen and induces a signal in the detection coils. The magnitude and phase of this signal is determined by a phase-sensitive amplifier and is shown in Fig. 2 for a Nb specimen. The induced voltage increases linearly in the Meissner state and its phase remains constant. The induced-signal field dependence is determined for fixed vibrational amplitude driven at the acoustic resonant frequency of the specimen. Deviation from the linear field dependence occurs as the flux penetrates the specimen, resulting in a decrease in the dipole field. An additional signal is induced in the detection coils which result from eddy currents being generated in the normal regions of the specimen due to the relative acoustic motion of the specimen with respect to the field. This signal is observed to be 180° out of phase with the dipole signal. As more material becomes normal the eddy-current signal approaches the size of the dipole voltage and their vector sum becomes a minimum which is accompanied by a phase shift of 180°. Above H_{c2} the eddy-current signal is linear with increasing field.

Measurements are made at two fixed temperatures of 4.2 and 1.8°K as a function of applied magnetic field. The fractional change in elasticity is determined in parts per million by observing the magnetic field dependence of Young's modulus through measurements of the resonant frequency of the specimen. A summary of the properties of the specimens used in this investigation is given in Table I. The residual resistance is determined by a four-probe method with measurements at 4.2° performed in magnetic fields sufficient to drive the specimen into the normal state. The superconducting surface sheath is observed in some specimens with the ratio of H_{c2} to H_{c3} in agreement with that observed by Webb.[10] The high-field ($>H_{c3}$) magnetoresistance[11] is extrapolated to zero field to obtain the residual resistance. Vacuum annealing near the melting point of Nb increases the resistance ratio but can also "increase" the residual resistance. To obtain an indication of the relative mean free paths of the normal-state electrons in different specimens, the residual resistivities rather than the resistance ratios (Γ) are compared.

TYPE-I SUPERCONDUCTORS

The stiffness of solids in general decreases as a result of transition to the superconducting state. The change in elastic modulus is small and temperature-dependent. Young's modulus for Ta below the transition temperature is less in the superconducting state ($H=0$) than the normal state ($H>H_c$) by a few parts per million (Fig. 3). Of particular interest in this investigation is the behavior of the solids in the superconducting state when magnetic flux penetrates the material.

The transition from superconducting to normal state can be induced over small magnetic field intervals in type-I materials of a particular geometry, while for any type-II materials this field region is always of finite extent. Since the elastic behavior in the transition region is of particular interest, the specimen geometry and field orientation are chosen to expand the magnetic field interval of the transition and establish a well-defined intermediate state in the type-I materials. The form of the specimen and the magnetic-field orientation lead to a demagnetization factor of $\frac{1}{2}$ with flux penetrating the bulk at one-half the critical field H_c.

The elasticity is independent of the external field in the Meissner state, where the magnetic field is excluded from the bulk of the material. An increase in elasticity is observed only at fields above $\frac{1}{2}H_c$ as a result of the initial flux penetration into the bulk of the specimen. The increase in stiffness is almost exclusively due to the transition from the superconducting state. Changes in stiffness resulting from the field of magnitude H_c

TABLE I. Specimen characteristics.

		Major impurity[a] (ppm)	Residual resistance ($\mu\Omega$ cm) 4.2°K	Resistance ratio $\rho_{300}/\rho_{4.2}=\Gamma$
Nb	Polycrystal	100 Ta	0.321	47
	Single crystal I	100 Ta	0.669	30
	Single crystal II	100 Ta	0.233	67
Ta	Polycrystal	25 Nb, 10 C	2.12	20
	Single crystal	25 Nb, 10 C	0.20	147
V	Polycrystal	112 O, 20 Fe, 12 Ni	1.25	17

[a] As reported by the Materials Research Corporation.

[10] G. W. Webb, Solid State Commun. 6, 33 (1968).
[11] E. Fawcett, W. A. Reed, and R. R. Soden, Phys. Rev. 159, 533 (1967).

through the normal-state regions[12] are much smaller than the observed changes due to the superconducting transition and are ignored in the following. The stiffness change is not reversible in magnetic fields decreasing from above H_c and residual stiffness remains at zero field. The trapped flux leading to residual stiffness escapes as the temperature is raised above the critical temperature, resulting in the return of the normal-state elasticity. Reproducibility of these characteristic elastic parameters after cycling above the critical temperature is limited only by the accuracy of the measurement indicating no appreciable thermal hysterisis.

The field dependence of the stiffness of a single crystal of Ta (Fig. 4) exhibits behavior similar to the polycrystalline material. The fractional change in stiffness varies linearly with applied magnetic field between $\frac{1}{2}H_c$ and H_c. A residual stiffness associated with trapped flux is also noted. The magnitude of the total change in stiffness, however, is larger in the single crystal than in the polycrystalline material. The resudual resistance at 4.2°K is smaller for the single crystal, indicating a longer mean free path for the normal-state electrons. Correlation of the longer mean free paths with the larger values of the total change in stiffness is noted in all the materials investigated (both types-I and -II). The elastic properties of materials are apparently modified in the superconducting state through a shielding process which is dependent on scattering parameters analogous to those affecting the electrical transport properties. The shielding has a higher efficiency with the longer coherence of the superconducting quasiparticles. This effect is discussed in more detail in a later section.

The linear magnetic field dependence of the elasticity in the intermediate state suggests a rather uncom-

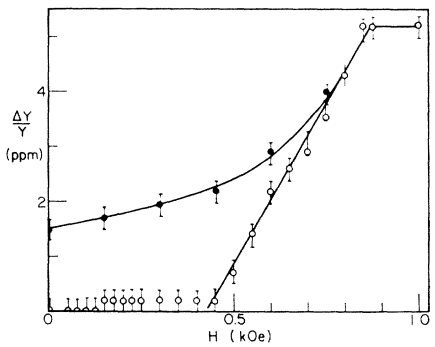

FIG. 3. Magnetic field dependence of the fractional change in elasticity (Young's modulus) in parts per million of a polycrystalline Ta rod. Open circles correspond to increasing field values and the filled circles to decreasing field values. The elasticity begins to increase at $\frac{1}{2}H_{c1}$ and reaches a maximum at H_{c1}. A hysterisis results in a residual stiffness associated with trapped flux which disappears when the temperature is raised above the critical temperature. The elasticity is determined at a temperature of 1.8°K.

[12] J. N. Lange, Phys. Rev. **179**, 631 (1969).

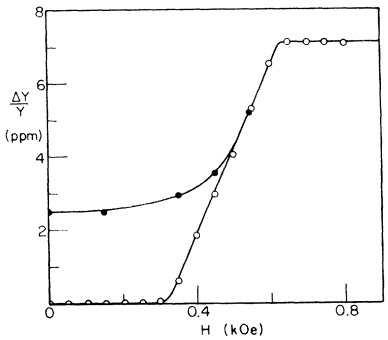

FIG. 4. Magnetic field dependence of the fractional change in stiffness at 1.8°K for a Ta single crystal. The acoustic displacement is along the [100] direction, while the magnetic field is in the [110] direction. The total change in stiffness is larger than in the polycrystalline tantalum.

plicated form for the contribution of the superconducting and normal-state regions to the total stiffness. All the type-I materials investigated, which include Pb and Sn in addition to Ta, exhibited this linear field dependence of the stiffness. The total stiffness in the intermediate state is assumed to be the sum of components from the normal and superconducting regions of the specimen. Similar approximations are made in determining the net magnetic moment in the intermediate state. The fractional change in elasticity is then proportional to the relative volume of the normal and superconducting regions as the increasing external magnetic field drives the specimen into the normal state and is given by

$$\Delta Y/Y = (\Delta Y/Y)_T V_N(H)/V_0, \qquad (1)$$

where $(\Delta Y/Y)_T$ is the total fractional change of the stiffness between the superconducting and normal state, V_0 is the volume of the specimen, and $V_N(H)$ is the normal-state field-dependent volume of the intermediate state. The normal-state volume calculated using Eq. (1) and Figs. 3 and 4 exhibits a linear dependence of external field in the intermediate state. In contrast, the elastic behavior of type-II materials in the mixed state is considerably more complicated and indicates that interactions between normal regions are important.

TYPE-II SUPERCONDUCTORS

Type-II superconductors exhibit a mixed state in which flux penetrates the material at fields above a lower critical field H_{c1}, independent of the geometry of the superconductor. The normal state returns above a second critical field H_{c2}. The negative surface energy between the superconducting and normal regions leads to flux entering the bulk in quantized units in the form of a filament surrounded by circulating supercurrents. Because of the analogy to superfluid flow, this configuration is referred to as a vortex.

The elastic properties of type-II materials reflect the transition form the Meissner to the normal state as for

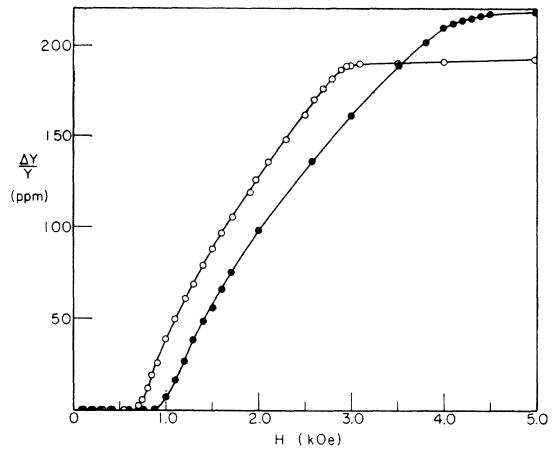

FIG. 5. Field dependence of the fractional change in elasticity for a Nb single crystal at 4.23 (open circles) and 1.73°K (closed circles). The acoustic displacement is along the [110] direction, while the field is in the [100] direction.

type-I superconductors, but with a considerably more complicated field dependence. The experimental configuration uses specimens of the same geometry and identical magnetic field orientations as in the study of the type-I materials, but the fractional change in elasticity does not exhibit a linear dependence on the external magnetic field as observed for the type-I materials. The field dependence of the transition to the normal state is illustrated by the elastic changes in Nb (Fig. 5) and V (Fig. 6). Only at magnetic fields below H_{c1} (remembering a demagnetization factor of $\frac{1}{2}$) is a linear increase in the fractional change in elasticity noted. A crude calculation of the number density (number per area) of vortices in Nb at 1.8°K, assuming each vortex contains a flux of ϕ_0, needed to construct a field of H_{c1} near the surface of the specimen, gives a value of $\sim 10^{10}$ vortices per cm^2. If the structure of the vortex is assumed to be that suggested by Caroli, de Gennes, and Matricon,[8] the vortex incorporates a normal core surrounded by circulating supercurrents. The radius of the core is ξ_0, the coherence length for high-purity Nb is 450 Å as determined by Finnemore, Stromberg, and Swenson.[13] The vortices are then separated by only 900 Å in an external field of H_{c1}. Since the penetration depth λ is approximately 480 Å, an appreciable interaction between vortices occurs due to the proximity of the nearest neighbors. This results in a more complicated elastic behavior in the mixed state than noted for type-I materials in the intermediate state. Similar numerical arguments can be made for V from the values of ξ_0 and λ determined by Radenbaugh and Keesom.[14]

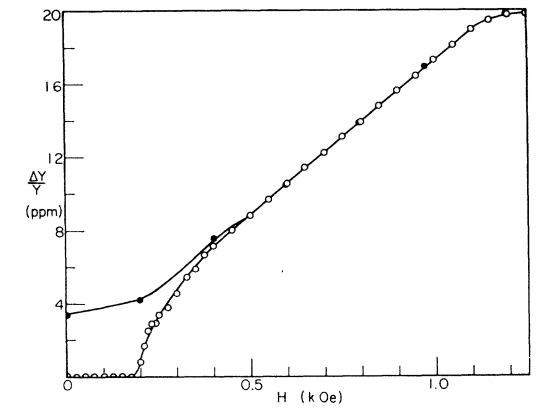

FIG. 6. Field dependence of the fractional change in elasticity for polycrystalline vanadium at 4.2°K.

In order to describe the field dependence of the elasticity in terms of parameters associated with the mixed state, it is again assumed that the total elasticity is the sum of contributions due to normal and superconducting regions. The fractional change in elasticity is given by Eq. (1), where $(\Delta Y/Y)_T$ is the total fractional elastic change in the type-II materials. The normal-state field dependence of the elasticity[12] in fields slightly larger than H_{c2} is negligible compared to the superconducting transition and is ignored in the following.

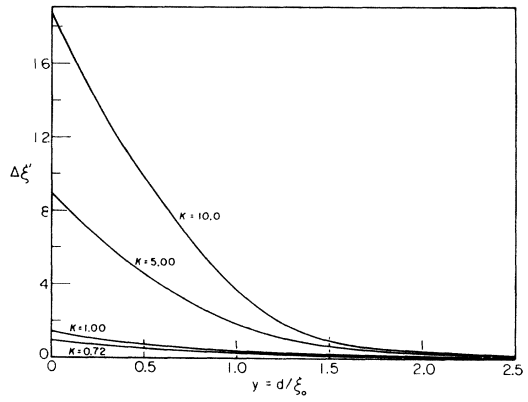

FIG. 7. The fractional increase in the radius of the vortex as a function of the vortex separation d normalized to the coherence length $y=e/\xi_0$. The interaction is significant over larger distances for the more extreme type-II materials. The curves are computed from Eq. (5).

The observed field dependence of the elasticity, through its dependence on the normal volume, can be used to determine the separation and number of vortices as a function of magnetic field within the framework of a model of the vortex and its interactions. The results are not critically dependent on the detailed shape of the vortex, since the net elasticity depends on the volume. The fractional change in modulus Eq. (1) can be expressed in terms of the density of vortices (n) and total area of the core (A_c) as

$$\Delta Y/Y=[\Delta Y/Y]_T nA_c. \qquad (2)$$

[13] D. K. Finnemore, T. F. Stromberg, and C. A. Swenson, Phys. Rev. **149**, 231 (1966).
[14] R. Radebaugh and P. H. Keesom, Phys. Rev. **149**, 217 (1966).

A convenient model of a vortex[8] incorporates a normal core surrounded by circulating supercurrents. If the vortex is isolated and does not interact with its neighbors, the diameter of the normal core is twice the coherence length $2\xi_0$. The magnetic field in the normal core assumes a minimum value of $H_{c2}=\phi_0/4\xi_0^2$. The magnetic field external to the normal core decreases exponentially into the superconducting regions, as suggested by the London equations.

A stable configuration of interacting vortices is assumed to minimize the energy density in its normal core to an average value of $H_{c2}^2/8\pi$ as it is for isolated vortices. As the vortices approach each other, the overlap of the magnetic field of the nearest neighbors increases, resulting in the area of the normal core of the vortex increasing to maintain an energy density of $H_{c2}^2/8\pi$. The magnetic field inside the expanded core remains H_{c2}, and the total flux in the core becomes

$$H_{c2}\xi^2=H_{c2}\xi_0^2+\int_c H(r)dS, \tag{3}$$

where ξ is the expanded dimension of the interacting

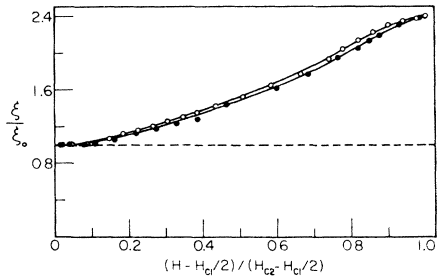

FIG. 8. The change in normalized radius of the vortex as a function of field in the mixed state. The reduced field variable is zero at $\frac{1}{2}H_{c1}$ and 1 at H_{c2}. The points are compiled from Fig. 5 and Eq. (8) for $\kappa=1$.

vortex whose original and minimum dimension is ξ_0. The integral is over the core and contributes flux due to the field of the neighboring vortices $H(r)$. To evaluate the integral of Eq. (3), a model of the core is chosen which minimizes computational difficulties and still retains the salient features suggested by de Gennes.[8] The cross section of the core is assumed to be square with sides of 2ξ length. The core is in the normal state and contains a magnetic field of H_{c2}. The magnetic field exterior to the normal core decreases as

$$H(r)=H_{c2}e^{-r/\lambda} \tag{4}$$

in the surrounding superconducting region. This form is dictated by the solution of the London equations for field penetration at a plane superconducting boundary. The parameter λ is the London penetration depth.

The transcedential equation resulting from the solution of Eq. (3) relates the fractional increase in size of the vortex ($\Delta\xi'$) with its distance d from its

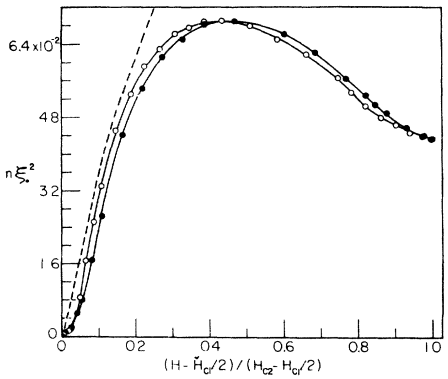

FIG. 9. Density of vortices (number per area) as a function of magnetic field. The points are compured for the two temperatures of Fig. 8 from Eq. (6). The dashed curve is computed using a nonexpanding vortex of dimensions $2\xi_0$.

four nearest neighbors. It is given by

$$\left(1+\Delta\xi'-\frac{1}{1+\Delta\xi'}\right)\left(\frac{e^{-2/\kappa}}{e^{-2\kappa}-e^{-2\Delta\xi_0/\kappa}}\right)=2e^{-d/\xi_0\kappa}, \tag{5}$$

where κ is the Landau-Ginsburg parameter.

The solution to Eq. (5) for various Landau-Ginsburg parameters is shown in Fig. 7 as a function of separation d between neighboring vortex boundaries. The more extreme type-II materials undergo long-range interactions between the vortices. The expansion of the core of the vortex becomes significant at much greater distances than in materials with small κ. The density n (number per area) of expanded vortices is

$$n=1/[2\xi_0(1+\Delta\xi')+d]^2, \tag{6}$$

while the area of the core A_c is

$$A_c=4\xi_0^2(1+\Delta\xi')^2, \tag{7}$$

giving a form for the fractional change in elasticity as

$$\frac{\Delta Y}{Y}=\left(\frac{\Delta Y}{Y}\right)_T\frac{4\xi_0^2(1+\Delta\xi')^2}{[2\xi_0(1+\Delta\xi')+d]^2}. \tag{8}$$

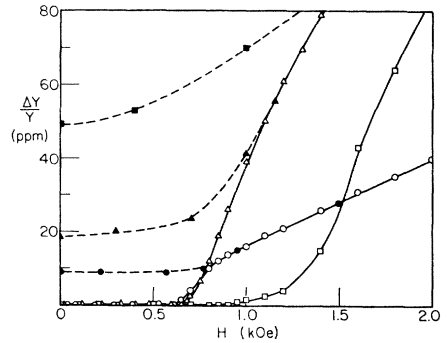

FIG. 10. The field dependence of the fractional change in stiffness for two single crystals (circles, RRR=30; triangles, RRR=67) and a polycrystal (rectangle, RRR=47) of Nb. The open points are for increasing field and the closed points for decreasing field. The residual stiffness is isotropic and reproduces to the accuracy of the measurement in all the samples.

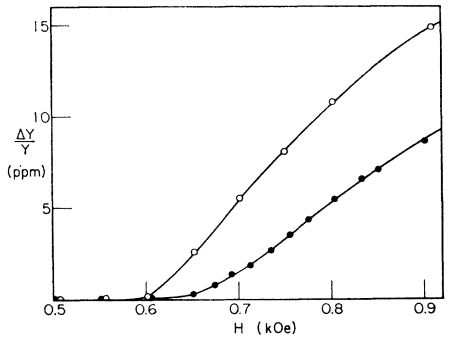

FIG. 11. Magnetic field dependence of the fractional change in elasticity for a single crystal of niobium at 4.23°K. The magnetic field scale is expanded in the vicinity of $\frac{1}{2}H_{c1}$. The changes in electricity above the Meissner state are anisotropic as shown for the two different magnetic field orientations (open circles—[110], closed circles—[100]).

This result [Eq. (8)] is applied to the observed field dependence of the elasticity to obtain the size ξ and density n of the vortices as a function of external magnetic field. The field dependence of the normalized size of the vortex ξ/ξ_0 is determined by use of $\kappa=1$ and Eq. (6) (see Fig. 8). If there is no interaction between the vortices, no expansion of the vortex would occur, and the width of, the vortex would be given by the dashed line. The overlap of the fields of the nearest neighbors leads to an appreciable expansion of the vortex at fields above H_{c1}. The vortex expands with increasing field to a finite value at H_{c2}. The field dependence of the vortex size is temperature-independent on a reduced field plot, as would be expected, since the details of the mixed state would primarily be field-independent at temperatures much below T_c. The validity of the model of the vortex is obviously limited in the high-field region, since the shape of the vortex most probably is severely distorted. The density of vortices (Fig. 9) is asymptotic to the rigid vortex density (dashed curve) at very low fields but deviates significantly from this value at fields above H_{c1}. The density goes through a maximum at intermediate field regions and then decreases with further increases in field. Since the bulk area of the specimen is constant, the decrease in vortex density leads to a decrease in the number of vortices penetrating the bulk at the higher fields. For fields near H_{c2}, the rate of expansion of the area of the vortex becomes more rapid than the corresponding decrease in separation of the edges of the vortices with a net effect of decreasing the number threading the superconductor. Within the limits of the model of the vortex, the elasticity can be used to determine the size, separation, and density of vortices throughout the mixed state.

RESIDUAL STIFFNESS

As the external magnetic field decreases below H_{c2} the flux is expelled from the bulk of the material, and the stiffness decreases in the mixed state. The original value of the stiffness is not reached again in the Meissner state, but a hysterisis resulting in a residual stiffness (Fig. 10) in zero field is observed. The residual component disappears at temperatures above T_c. The hysterisis becomes apparent at relatively low fields ($<H_{c1}$) for which the separation of the vortices is increasing rapidly. The residual stiffness is attributed to flux being trapped by imperfections and impurities in the bulk. At fields above H_{c1} the vortices are closely spaced and their mutual repulsion is larger than any pinning effects, with their behavior determined primarily by the external field. As the external field decreases and the vortex separation increases, the mutual repulsion can become less than the attractive pinning forces of the imperfections, thus immobilizing the remaining vortices.

The residual stiffness observed in a polycrystalline specimen is considerably higher than that of the two single crystals shown in Fig. 11. The residual resistance of the polycrystalline material is between those of the single crystals, even though it most probably possesses a much larger imperfection density than either of the single crystals. The higher residual stiffness in the polycrystalline material indicates the grain boundaries or associated dislocation substructure are more effective in trapping flux than the impurities. The separation and density of the vortices can be determined by the calculation outlined in a previous section to the magnitude of the residual stiffness. The results of this analysis are given in Table II for a high-purity Nb single crystal. The surface is strongly etched before each measurement,[15] and the reproductibility of the residual stiffness is equal to the accuracy of the measurement.

The residual stiffness exhibits a temperature dependence but no appreciable anisotropy. The trapped vortices are more tightly bound to the imperfections at the higher temperatures as reflected in the larger residual stiffness at 4.2 than at 1.8°K. The trapped vortices exist with a higher density and closer separation at the higher temperature. A mechanism which would bind the vortices more tightly at higher temperatures is not obvious, since increased thermal motion of the dislocations would seem to shed the vortices more readily than pin them if only elastic coupling[16,17] were effective. It appears that the interaction of the vortex

TABLE II. Separation and density of trapped vortices which lead to a residual stiffness.

	Residual stiffness (ppm)	Temperature (°K)	Vortex separation [units of $1/\xi(T)$]	Vortex density n [units of $10^{-2}\,\xi(T)$]
Nb II	18.5	4.2	4	2.75
	12	1.8	6	1.75

[15] R. B. Flippen, Phys. Letters **24A**, 588 (1967).
[16] E. J. Kramer and C. L. Bauer, Phil. Mag. **15**, 1189 (1967).
[17] W. W. Webb, Phys. Rev. Letters **11**, 191 (1963).

with imperfections, involves more than simply the elastic coupling. Indeed, it may include electromagnetic terms reflecting the thermal motion of the pinning configuration.

SUPERCONDUCTING PROPERTIES OF Nb

Because the elasticity is a bulk property of the solid, its behavior is useful in determining parameters of the superconducting state, such as the critical fields. Nb is particularly suited for such a study using a resonant technique, since its attention is very small at low temperatures ($Q^{-1}\sim 10^{-7}$) with a resulting high resolution of the resonance frequency. The attenuation of Nb is temperature-dependent in the superconducting state, and relaxation peaks are observed similar to those seen by Kramer and Bauer.[6]

Field-dependent changes in the elasticity indicate, to a high degree of accuracy, both critical fields in type-II superconductors. The elastic wave propagates along the axis of the cylindrical specimens with an almost constant-stress distribution over the cross section. The velocity of the wave, and thus the resonance frequency of a finite cylinder, is dependent on the elastic stiffness averaged over the cross section of the cylinder and not on detail surface properties which are so critical to measurements of electrodynamic properties such as the magnetization. In the Meissner state, no field dependence of the elasticity is observed since the flux does not penetrate the bulk of the superconductor. At one-half the first critical field ($D=\frac{1}{2}$) the flux begins to penetrate and the stiffness increases. In a Nb single crystal the first critical field is observed to have a small but measurable anisotropy as seen in Fig. 11. The flux penetration for the magnetic field in the [100] direction occurs approximately 30 Oe below the value for the field in the [110] direction. Anisotropies in the first critical field are readily detected by elasticity changes which occur rapidly as the flux penetrates, in contrast to the more gradual change in slope exhibited in magnetization measurements.

The upper critical field H_{c2} is determined in a similar manner. The field idependence of the elasticity is very small above H_{c2} on the scale of the superconducting transition, while the change in elasticity immediately

TABLE III. Critical fields for Nb determined from changes in elasticity.

	Field direction	H_{c1} (kOe)	H_{c2} (kOe)	Temperature (°K)
Single crystal I	[100]	1.34	3.49	4.2
$\Gamma=30$	[110]	1.24	3.28	4.2
Single crystal II	[100]	1.32	2.95	4.2
$\Gamma=67$	[111]		2.97	4.2
	[100]	1.73	4.05	1.8
	[111]	1.85	4.20	1.8
Polycrystal $\Gamma=47$		1.90	3.15	4.2

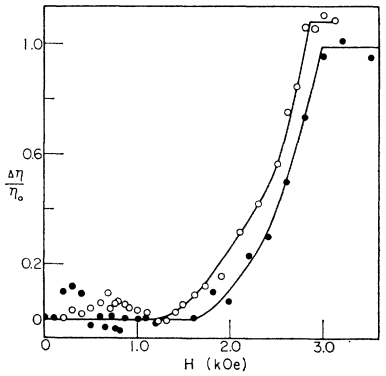

FIG. 12. Fractional change in loss factor η as a function of magnetic field at 4.23°K. The second critical field is lower for the magnetic field in the [100] direction (open circles) than in the [111] direction (closed circles).

below H_{c2} is relatively rapid when presented on a logarithmic scale. The intersection of straight lines drawn through points immediately above and below H_{c2} serve to define the critical field. An anisotropy is noted in the single-crystal Nb which is consistent in direction and magnitude with values determined by magnetization measurements[18,19] (see Table III).

The attenuation is small in Nb at low frequencies and cannot be determined as accurately as the stiffness. The field dependence of the fractional change in attenuation is shown in Fig. 12 for the field in the [100] and [110] directions in a single crystal of Nb. No appreciable change in the attenuation is noted until fields well above H_{c1}. The attenuation then increases rapidly to the normal-state value in a manner similar to observations at ultrasonic frequencies.[20] The anisotropy noted in the second critical field determined by the stiffness is apparent also in the attenuation.

NONLOCAL SCREENING

The reduction in stiffness resulting from the superconducting transition can be viewed as an increased screening of the lattice-ion interactions by the superconducting quasiparticles. The effectiveness of the additional shielding is observed to depend on the mean free path of the normal electrons. The total change in elasticity is always larger for the longer mean free paths for both type-I (Ta) and -II (Nb) materials. No dependence of the total change in elasticity is noted for effects which do not influence the mean free path of the normal electrons such as the specimen geometry.

The relationship between the total change in elasticity and resistivity, observed to be temperature-independent at temperatures well below T_c, has the

[18] C. E. Gough, Solid State Commun. 6, 215 (1968).
[19] D. E. Farrell, B. S. Chandrasekhar, and S. Haung, Phys. Rev. 176, 562 (1968).
[20] T. Tsuneto, Phys. Rev. 121, 402 (1961).

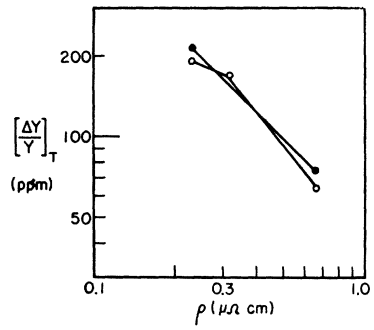

FIG. 13. Logarithm of the total fractional change in Young's modulus of Nb due to the superconducting transition as a function of residual resistance. Open circles correspond to elasticity measurements at 4.2 and closed circles at 1.8°K.

form

$$Y_s = Y_n C\rho^m/(1+C\rho^m), \tag{9}$$

where Y_s is the Young's modulus in the superconducting state, Y_n is the normal-state modulus, and ρ is the resistivity. The observed behavior for three different Nb specimens is shown in Fig. 13. The resistivity can be expressed in terms of a constant D and the electron mean free path l, Eq. (9) then becomes

$$Y_s = \frac{Y_n}{(l^m/D^m C+1)}, \tag{10}$$

where D is proportional to the number of charge carriers, the Fermi velocity, the electronic charge, and the effective mass. Empirical values for m and C for Nb and Ta are given in Table IV.

The superconducting quasiparticles are scattered[21] by imperfections similar to those which scatter the normal electrons. Screening of the lattice interactions appears to be most effective when the lifetime between scatterings, during which the electron pairs move coherently is longest. The influence of the coherence of the quasiparticles on their screening effectiveness is analogous to the nonlocal electromagnetic interactions introduced by Pippard[22] to obtain the correct magnitude of the penetration depth in high-purity type-I materials.

TABLE IV. Empirical values for m and C of Nb and Ta.

	m	C [10^{-10} (Ω cm)$^{-1}$]
Nb	0.97	0.022
Ta	0.13	0.175

[21] J. Bardeen, in *Low Temperature Physics*, edited by R. Davies (Butterworths Scientific Publications, Inc., Washington, D. C., 1963), p. 7.

CONCLUSIONS

The magnetic field dependence of the elasticity is related to the relative normal and superconducting volumes. For type-I superconductors, the normal volume is determined to be a linear function of the magnetic field in the intermediate state. The elastic behavior in the mixed state of type-II materials is more complicated than for type-I materials. Interactions between vortices in type-II materials result because of their high density in the mixed state. These interactions lead to a change in vortex density and an expansion of its normal core in fields above H_{c1}. The field dependence of the elastic changes is used to compute the size and density of vortices as a function of magnetic field. The density is found to decrease at fields near H_{c2} where the expansion of the vortex is more rapid than the decrease in separation relative to its neighbors.

A hysterisis in the field dependence of the elasticity results in a residual stiffness at zero field due to vortices pinned by imperfections. The temperature dependence of the pinning force indicates interactions, in addition to those associated with elastic gradients, are needed to characterize vortex pinning. These interactions may be of electromagnetic origin.

The total change in stiffness resulting from the superconducting transition is observed to be proportional to the mean free path of the normal electrons. The shielding of the interactions of the lattice ions apparently is more effective for the longer coherence of the superconducting quasiparticles.

Elastic measurements on Q-high materials are an accurate means of determining the bulk critical fields for superconductors. The measurements, relatively independent of surface effects and coupled with simultaneous determinations of the magnetization, offer a reliable means of differentiating between bulk and surface properties of superconductors.

[22] A. B. Pippard, Proc. Roy. Soc. (London) **A216**, 547 (1953).